Genomic Profiling Reveals *Pitx2* Controls Expression of Mature Extraocular Muscle Contraction–Related Genes

Yuefang Zhou,[1] *Bendi Gong,*[2] *and Henry J. Kaminski*[3]

Purpose. To assess the influence of the Pitx2 transcription factor on the global gene expression profile of extraocular muscle (EOM) of mice.

Methods. Mice with a conditional knockout of *Pitx2*, designated $Pitx2^{\Delta flox/\Delta flox}$ and their control littermates $Pitx2^{flox/flox}$, were used. RNA was isolated from EOM obtained at 3, 6, and 12 weeks of age and processed for microarray-based profiling. Pairwise comparisons were performed between mice of the same age and differentially expressed gene lists were generated. Select genes from the profile were validated using real-time quantitative polymerase chain reaction and protein immunoblot. Ultrastructural analysis was performed to evaluate EOM sarcomeric structure.

Results. The number of differentially expressed genes was relatively small. Eleven upregulated and 23 downregulated transcripts were identified common to all three age groups in the *Pitx2*-deficient extraocular muscle compared with littermate controls. These fell into a range of categories including muscle-specific structural genes, transcription factors, and ion channels. The differentially expressed genes were primarily related to muscle contraction. We verified by protein and ultrastructural analysis that myomesin 2 was expressed in the *Pitx2*-deficient mice, and this was associated with development of M lines evident in their orbital region.

Conclusions. The global transcript expression analysis uncovered that Pitx2 primarily regulates a relatively select number of genes associated with muscle contraction. Pitx2 loss led to the development of M line structures, a feature more typical of other skeletal muscle. (*Invest Ophthalmol Vis Sci.* 2012;53:1821–1829) DOI:10.1167/iovs.12-9481

The extraocular muscles (EOMs) have adapted a unique molecular expression pattern, to an extent that some have argued EOM to be classified as a specific allotype as are cardiac, smooth, and skeletal muscles.[1] Its unique properties are driven by the requirements of the visual system for rapid, coordinated eye movements, which resist fatigue. The maintenance of the mature EOM phenotype relies on cell-autonomous and non-cell-autonomous regulatory mechanisms. Dissection of these regulatory mechanisms may make it possible to exploit them to modify EOM contractile properties and influence eye movements, which could lead to improvements in treatment for strabismus and other disorders of ocular motility. In addition, appreciation of phenotypic regulation may improve understanding of disease characteristics, such as the sparing of EOM by most muscular dystrophies and their preferential involvement by orbital myositis and myasthenia gravis.[2]

The regulation of the molecular signature of the EOM is not understood, but is influenced by extrinsic influences, such as innervation,[3] stretch,[4,5] thyroid hormone,[6] and intrinsic properties. Pitx2, a bicoid-like homeobox transcription factor[7–10] is an intrinsic controller of EOM development and targeted deletion of *Pitx2* in mice by homologous recombination leads to agenesis of EOM.[7,11] We have also determined *Pitx2* to be a key regulator of the mature phenotype.[12,13] Pitx2 is expressed in adult rodent EOM at high levels,[12,14,15] and its conditional knockout at about P0 produces EOM without obvious pathology. The conditional knockout of *Pitx2* occurs at a time when EOM is continuing to undergo postnatal development including refinement of its mature innervational and myosin expression patterns.[12,13] However, alterations occur in key characteristics: (1) The *Pitx2*-deficient EOM are stronger, faster, but more fatigable. (2) The characteristic multiple innervation of certain fibers is lost. (3) Expression of myogenic regulatory factors such as myogenin, Myf5, and MyoD is dramatically downregulated. (4) Gene transcripts and protein levels of *Myh6*, *Myh7*, and *Myh13* isoforms are downregulated, whereas the longitudinal and cross-sectional patterns of expression of 2A-MyHC and 2X-MyHC isoforms are altered.[12,13] Therefore, Pitx2 must influence several pathways that control the adult EOM phenotype.

In this study, we used gene microarray (Affimetrix, Santa Clara, CA) analysis to evaluate and identify downstream processes regulated by Pitx2 in EOM. A select number of genes encoding major contractile proteins, transcription factors, and ion channels were found to be differentially expressed in *Pitx2*-deficient mice.

Methods

Animals

Two mouse strains were crossed to generate the *Pitx2* conditional knockout mice: *muscle creatine kinase (MCK)-Cre* mouse strain and the $Pitx2^{flox/flox}$ mouse strain, as previously described.[12] Determination of the genotype was performed by PCR using genomic DNA isolated from tail tips. Mice that were both $Pitx2^{flox/flox}$ and *Cre* positive were referred to as the conditional knockout $Pitx2^{\Delta flox/\Delta flox}$ mice; their littermates, $Pitx2^{flox/flox}$ mice, were used as controls. Animals were maintained in accordance with National Institutes of Health (NIH) guidelines for animal care. All procedures involving mice were approved by Institutional Animal Use and Care Committees at Saint Louis University. All experiments were conducted in accordance with

From the [1]Department of Neurology and Psychiatry, Saint Louis University, St. Louis, Missouri; the [2]Department of Pediatrics, Washington University in St. Louis, St. Louis, Missouri; and the [3]Department of Neurology, Department of Pharmacology and Physiology, George Washington University, Washington, DC.

Supported in part by National Institutes of Health/National Eye Institute Grant R01 EY-015306 (HJK).

Submitted for publication January 12, 2012; revised February 7, 2012; accepted February 7, 2012.

Disclosure: **Y. Zhou**, None; **B. Gong**, None; **H.J. Kaminski**, None

Corresponding author: Henry J. Kaminski, Department of Neurology, George Washington University-MFA, 2150 Pennsylvania Ave, Washington, DC 20037; HKaminski@mfa.gwu.edu.

the principles and procedures established by the NIH and the Association for Assessment and Accreditation of Laboratory Animal Care and in the ARVO Statement for the Use of Animals in Ophthalmic and Vision Research.

Tissue Preparation

Extraocular rectus muscles were dissected at 3 weeks, 6 weeks, and 3 months of age from both *Pitx2*$^{\Delta flox/\Delta flox}$ and their littermates *Pitx2*$^{flox/flox}$ mice. Tissues were snap frozen in liquid N_2 and stored at −80°C until use. To minimize interlitter/animal variability, muscles were pooled from three mice for each of three independent replicates/age/muscle groups.

DNA Microarray

Isolation of RNA and preparation of labeled cRNA followed methods described previously.[15–17] Labeled cRNA was hybridized to mouse genome arrays (Affymetrix GeneChip Mouse Genome 430 2.0 Arrays; Fremont, CA), which interrogate 45,000 probe sets representing 39,000 unique transcripts and variants from over 34,000 well-characterized mouse genes. The manufacturer's standard posthybridization wash, double-stain, and scanning protocols used a fluidics station for washing and staining of arrays (Affymetrix GeneChip Fluidics Station 400 and GeneChip Scanner 3000).

Microarray Data Analysis

A commercial software suite (Affymetrix Microarray Suite [MAS], version 5.0) was used for initial data processing and fold ratio analyses. MAS evaluates sets of perfect match (PM) and mismatch (MM) probe sequences to obtain both hybridization signal values and present/absent calls for each transcript. We used the MAS filter to exclude transcripts that were absent from all samples for further analysis. Present calls for the samples range from 55.70% to 61.40%, with an average of 59.1 ± 0.01%. Any transcripts with expression intensity below 300 (fivefold the background level) across all the samples were also excluded since distortion of fold difference values results when expression levels are low and may be within the level of background noise. Pairwise comparisons were used. Transcripts defined as differentially regulated between *Pitx2*$^{\Delta flox/\Delta flox}$ and *Pitx2*$^{flox/flox}$ groups met the criteria of: (1) nine of nine increase/decrease calls each *Pitx2*$^{\Delta flox/\Delta flox}$ EOM versus *Pitx2*$^{\Delta flox/\Delta flox}$ EOM in three replicates with nine comparisons and (2) absolute value of the average fold difference value ≥2.0. Hierarchical clustering was performed using the clustering function in commercial software (GeneSpring; Agilent Technologies, Santa Clara, CA). All differentially regulated genes as a gene list and their expression levels were organized by both individual samples as well as groups. Transcript annotations (Affymetrix) were replaced with official gene nomenclature and functions were assigned using information in National Center for Biotechnology Information Entrez Gene, UniGene, and PubMed, and Affymetrix NetAffx and Weizmann Institute of Science GeneCards databases.

Quantitative Real-Time PCR Validation

Selected transcripts were reanalyzed by quantitative real-time PCR (qPCR), using the same samples as in the microarray studies. Quantitative PCR used a PCR core reagent (SYBR green) with a sequence detection system (PRISM 7500 Sequence Detection System; Applied Biosystems, Foster City, CA), as described previously.[12] Mouse GAPDH was used as an internal positive loading control; for primers, see supplemental Table S1. Fold change values represent averages from triplicate measurements, using the $2^{-\Delta\Delta CT}$ method.[18]

Western Blot Analysis

EOMs from each mouse were rinsed in cold PBS before being homogenized with a microfuge pellet pestle (Sigma, St. Louis, MO) in 300 μL of homogenization buffer: 250 mM sucrose, 100 mM KCl, 5 mM EDTA, 20 mM Tris plus 1× protease inhibitor cocktail (Sigma, St. Louis).[19] The homogenate was kept on ice with shaking for 30 minutes and then centrifuged for 15 minutes at 13,000*g* at 4°C. The supernatant was removed and the protein concentration was measured using the Bradford method.[20] Muscle lysates containing 20 μg of total protein were separated by SDS-PAGE (7.5% acrylamide). Proteins were electrotransferred to a polyvinylidene difluoride membrane. The membrane was blocked in 5% blotting-grade blocker (Bio-Rad, Hercules, CA) in Tris-buffered saline/Tween (TBST; 150 mM NaCl, 20 mM Tris, 0.1% Tween 20) for at least 1 hour before addition of goat anti-myomesin 2 antibody (1:300; Santa Cruz Biotechnology, Inc., Santa Cruz, CA) at 4°C overnight. After being washed three times with TBST, the membrane was incubated with anti-goat horseradish peroxidase conjugate (Sigma, St. Louis, MO) at 1:5000 dilution for 1 hour. Membranes were again washed three times with TBST, incubated with reagents from the enhanced chemiluminescent Western blotting detection system (GE Healthcare, Pittsburgh, PA) according to the manufacturer's instructions and exposed to double-emulsion film (classic Blue BX Film; MidSci, St. Louis, MO) to visualize the immunoreactive bands.

Ultrastructural Analysis

Electron microscopy was performed as described by Schneiter et al.,[21] with exceptions as noted. The EOMs were dissected from mice with eyeball attached and fixed overnight in 2% glutaraldehyde (with 0.1 M sodium cacodylate). The individual muscle was isolated from the eyeball and washed and postfixed in 1% osmium tetroxide for 30 minutes. Muscle was transferred to 1% uranyl acetate for 1 hour at room temperature, then dehydrated with ethanol and embedded in staining and embedding media (LX-112 resin; Polysciences Inc., Warrington, PA). Longitudinal sections of the orbital layers were cut and stained with 2% uranyl acetate followed by lead citrate electron-opaque stain (Reynolds). Sections were examined with an electron microscope (JEM-100 CX11; JEOL, Tokyo) at 80 kV.

Results

Microarray Data Analysis

To identify global patterns of gene expression regulated by *Pitx2* in the EOM of the mice, triplicate RNA samples were prepared and further processed for microarray hybridization from the conditional knockout *Pitx2*$^{\Delta flox/\Delta flox}$ mice and the control *Pitx2*$^{flox/flox}$ littermates at 3 weeks, 6 weeks, and 3 months time points. The expression profiling showed 15 upregulated (supplemental Table S2) and 27 downregulated (supplemental Table S3) transcripts at 3 weeks, 40 upregulated (supplemental Table S4) and 74 downregulated (supplemental Table S5) transcripts at 6 weeks, 55 upregulated (supplemental Table S6) and 130 downregulated (supplemental Table S7) transcripts at 3 months in *Pitx2*$^{\Delta flox/\Delta flox}$ EOM compared with *Pitx2*$^{flox/flox}$ EOM at the analogous time points. These genes fell into the following major categories: muscle structural genes, transcription factors, receptors and ion channels, extracellular matrix molecules, molecules involved in metabolisms, responses to stress, immune responses, signaling, and some unclassified molecules and expressed sequence tags. A total of 213 transcripts were found to be differentially expressed in the EOM between *Pitx2*$^{\Delta flox/\Delta flox}$ and *Pitx2*$^{flox/flox}$ mice, covering 3 weeks, 6 weeks, and 3 months time points.

Hierachical cluster analysis (Fig. 1) showed a distinct temporal change in expression pattern of the genes found to be differentially influenced by the loss of *Pitx2* expression. Over the period of 3 weeks to 3 months, EOMs of *Pitx2*$^{\Delta flox/\Delta flox}$ mice in comparison with the *Pitx2*$^{flox/flox}$ mice demonstrate a decreased expression in about two thirds of the differentially

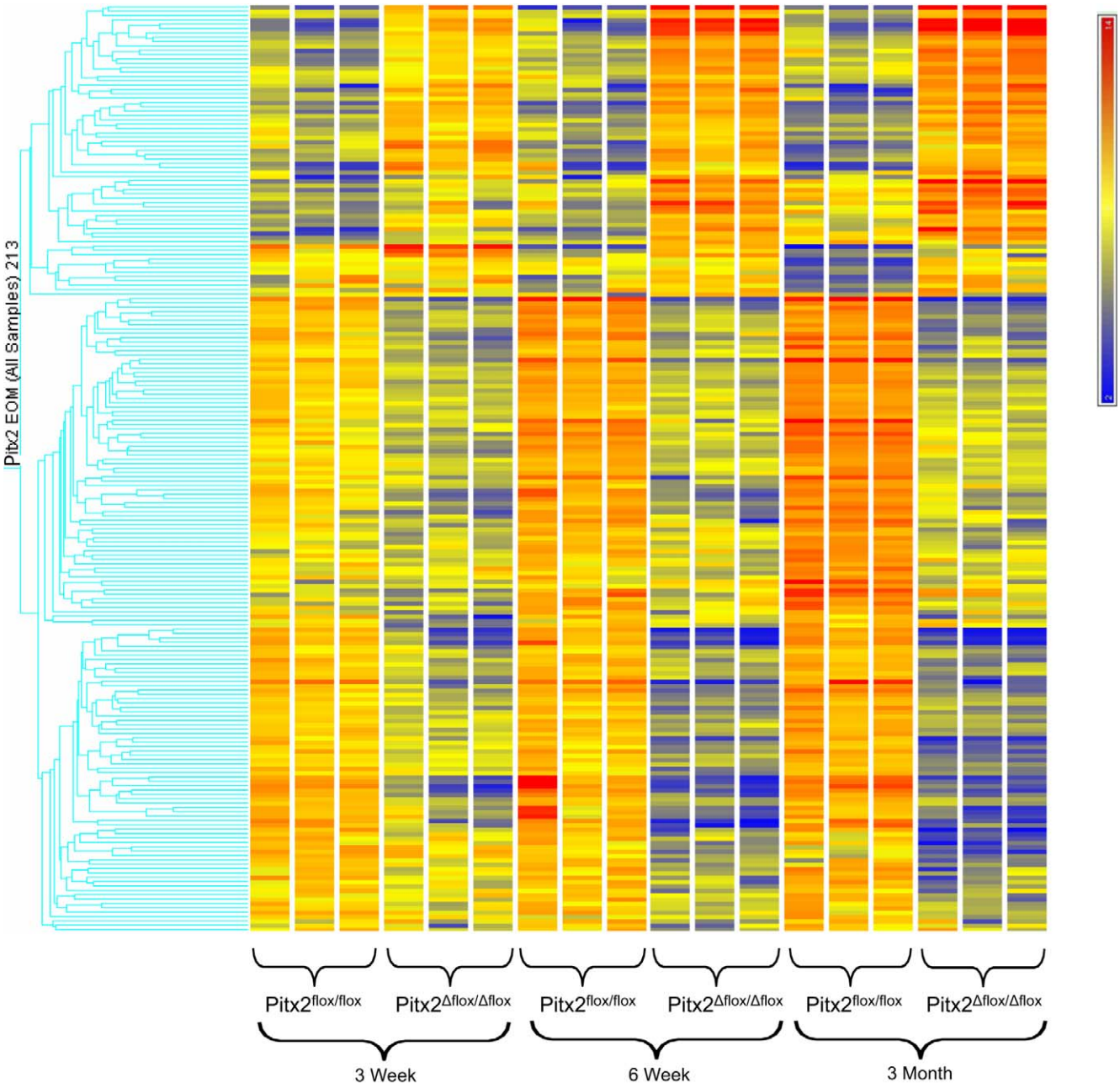

Figure 1. Hierarchical clustering of the gene probes identified as differentially expressed between extraocular muscles of *Pitx2*$^{\Delta flox/\Delta flox}$ and *Pitx2*$^{flox/flox}$ mice at 3 weeks, 6 weeks, and 3 months of age. Transcripts identified are those at the intersection of data obtained with the MAS and RMA algorithms (Affymetrix). The three independent replicates of each group are represented. The scale at the *top right* denotes normalized expression levels (*red*, high expression; *blue*, low expression).

expressed genes interrogated and an increase in expression of about one third of differentially expressed genes. The overall alteration of gene expression is also appreciated in Figure 2. Comparison of the differentially regulated transcripts across all three time points identified 12 upregulated transcripts (Table 1) and 23 downregulated transcripts (Table 2) common to all three time points. The majority of up- and downregulated genes were related to muscle contraction. Specific gene changes are discussed in the Discussion section.

Real-Time Quantitative PCR

Results of microarray gene expression evaluation were validated by qPCR for 13 select transcripts. The expression levels of four upregulated genes (*Kcne1l*, *Myom2*, *Ryr3*, and *Zmynd17)* and ten downregulated genes (Cacna2d4, Myh6, Myh7, Myl2, Pln, Psp, Tnnc, TnnI, Tnnt2, and Zfp533) were assessed. Expression changes were normalized to GAPDH expression. The qPCR analysis correlated well with the DNA microarray analysis (Table 3).

Immunohistochemical Analysis

Genomic profiling and qPCR identified myomesin 2 to be significantly upregulated at all three time points. Western blot analysis demonstrated that myomesin 2 protein was also increased in *Pitx2*$^{\Delta flox/\Delta flox}$ EOM (Fig. 3). Myomesin 2 is undetectable in the EOM of the wild-type *Pitx2*$^{flox/flox}$ mice,

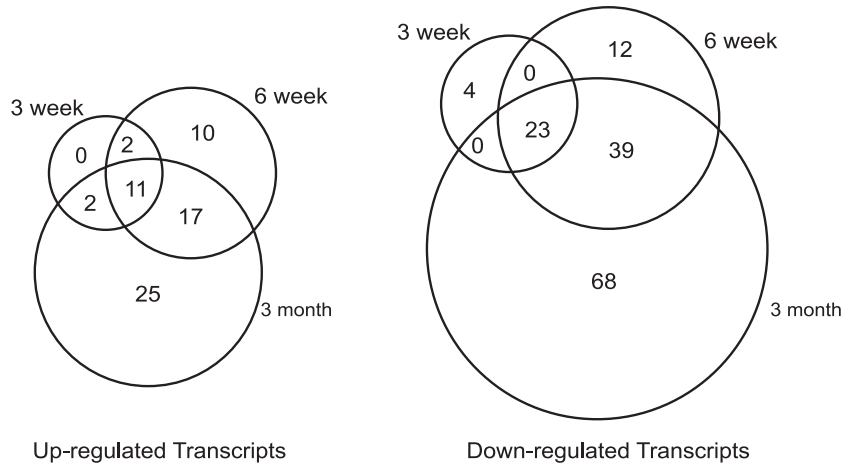

Figure 2. Venn diagram showing the numbers of differentially expressed transcripts between *Pitx2*$^{\Delta flox/\Delta flox}$ and *Pitx2*$^{flox/flox}$ EOM shared by or unique to the three time points.

whereas it is readily identified in extensor digitorum longus and heart. In contrast, in EOM from the *Pitx2*$^{\Delta flox/\Delta flox}$ mice, myomesin 2 is expressed at levels comparable to those of the extensor muscle. The upregulation of both transcript and protein levels of myomesin 2 prompted us to examine the ultrastructure of the sarcomere since myomesin 2 is one of the principal scaffolding components of M-lines, which cross-link the thick filaments of the sarcomere in place.[22,23] M-lines were present in the orbital layer of the *Pitx2*$^{\Delta flox/\Delta flox}$ EOM (Fig. 3C), whereas the M-lines were not detected in the *Pitx2*$^{flox/flox}$ EOM (Fig. 3B). The analysis was performed only on the orbital layers because of the much greater complexity of global layer fiber-type composition.[24]

Discussion

Our investigation demonstrates that Pitx2 in the immediate postnatal period controls a relatively select number of genes primarily involved in muscle contraction. The *Pitx2* conditional knockout EOM had a gradual decrease in expression of two thirds of the differentially expressed genes compared with *Pitx2*-sufficient EOM, suggesting that Pitx2 primarily acts through initiation of gene expression. Pitx2 was found to influence transcript levels of genes that are involved in characteristics that are a hallmark of wild-type EOM. The absence of Pitx2 led to the expression of myomesin 2 and return of M-lines to orbital fibers, a characteristic of other skeletal muscle.[25] Our previous studies demonstrated the loss of three unique characteristics of EOMs: (1) special MyHC isoform expression (α-cardiac MyHC, slow-MyHC, eom-MyHC, and slow-tonic MyHC), (2) the variation in longitudinal expression of many MyHC isoforms, and (3) multiinnervation.[12,13] Coupled with the present evaluations, we conclude that Pitx2 in the mature EOM is responsible for regulation of genes involved in establishment of unique aspects of EOM contractile properties.

Table 1. Transcripts Upregulated in *Pitx2*$^{\Delta flox/\Delta flox}$ EOM Compared with *Pitx2*$^{flox/flox}$ EOM Common to 3-week, 6-week, and 3-month Time Points

Accession No.	Gene Symbol	Gene Title	Go Biological Process Term	3w Fold Change	6w Fold Change	3m fold Change
BB288010	Myom2	myomesin 2	muscle contraction	4.6	8.4	14
BB474208	Myom2	myomesin 2	muscle contraction	5.0	14	16
AV241307	Myom2	myomesin 2	muscle contraction	4.7	9.8	16
AK014794	Zmynd17	zinc finger, MYND domain containing 17	—	5.4	22	18
BG069709	Zdhhc23	zinc finger, DHHC domain containing 23	—	2.3	3.4	3.7
AK004064	Dysfip1	dysferlin interacting protein 1	—	2.5	3.9	4.9
BM116248	Ctxn3	cortexin 3	—	2.6	4.3	6.5
NM_021487	Kcne1l	potassium voltage-gated channel, Isk-related family, member 1–like	ion transport	2.2	4.4	6.1
AV238793	Ryr3	ryanodine receptor 3	calcium ion transport /// striated muscle contraction /// transmembrane transport	3.2	4.3	6.6
X83934	Ryr3	ryanodine receptor 3	calcium ion transport /// striated muscle contraction /// transmembrane transport	3.2	5.8	7.9
AV337888	Pcp4l1	Purkinje cell protein 4–like 1	tricarboxylic acid cycle /// transport /// electron transport chain	2.3	3.1	2.8

Table 2. Transcripts Downregulated in *Pitx2*$^{\Delta flox/\Delta flox}$ EOM Compared with *Pitx2*$^{flox/flox}$ EOM Common to 3-week, 6-week, and 3-month Time Points

Accession No.	Gene Symbol	Gene Title	Go Biological Process Term	3w Fold Change	6w Fold Change	3m fold Change
NM_009393	Tnnc1	troponin C, cardiac/slow skeletal	regulation of muscle contraction /// regulation of muscle filament sliding speed /// regulation of ATPase activity	−3.7	−8.8	−12
NM_011619	Tnnt2	troponin T2, cardiac	regulation of muscle contraction /// muscle filament sliding /// regulation of ATPase activity	−4.1	−19	−11
L47552	Tnnt2	troponin T2, cardiac	regulation of muscle contraction /// muscle filament sliding /// regulation of ATPase activity	−3.9	−16	−8.8
BE952392	Myh7b	myosin, heavy chain 7B, cardiac muscle, beta	—	−2.9	−4.1	−3.4
NM_010861	Myl2	myosin, light polypeptide 2, regulatory, cardiac, slow	cardiac myofibril assembly /// ventricular cardiac muscle tissue morphogenesis /// heart contraction	−4.3	−7.9	−7.1
NM_080728	Myh7	myosin, heavy polypeptide 7, cardiac muscle, beta	muscle contraction /// muscle filament sliding /// ventricular cardiac muscle tissue morphogenesis	−3.1	−6.5	−10
M76601	Myh6	myosin, heavy polypeptide 6, cardiac muscle, alpha	regulation of the force of heart contraction ///muscle contraction /// striated muscle contraction /// regulation of heart contraction	−6.4	−14	−6.3
BB481540	Myh6 /// Myh7	myosin, heavy polypeptide 6, cardiac muscle, alpha /// myosin, heavy polypeptide 7, cardiac muscle, beta	regulation of the force of heart contraction /// striated muscle contraction	−3.4	−20	−7.0
NM_021467	Tnni1	troponin I, skeletal, slow 1	regulation of muscle contraction /// ventricular cardiac muscle tissue morphogenesis	−5.6	−18	−24
BB772205	Enho	energy homeostasis associated	—	−2.6	−4.1	−5.2
BB772205	Enho	energy homeostasis associated	—	−2.3	−4.5	−5.7
AK005148	Cyfip2	cytoplasmic FMR1 interacting protein 2	apoptosis /// apoptosis /// cell adhesion /// cell-cell adhesion /// cell-cell adhesion	−2.0	−2.6	−2.4
BB333374	Zfp385b	zinc finger protein 385B	—	−2.7	−5.1	−6.2
BE982894	Zfp385b	zinc finger protein 385B	—	−2.8	−4.5	−5.0
AK002622	Pln	phospholamban	regulation of the force of heart contraction /// calcium ion transport /// regulation of calcium ion transport	−3.0	−4.8	−3.3
AI426503	Mfsd4	major facilitator superfamily domain containing 4	transport /// transmembrane transport	−2.3	−3.5	−2.6
BB278653	Cacna2d4	calcium channel, voltage-dependent, alpha 2/delta subunit 4	transport /// ion transport /// calcium ion transport /// visual perception /// response to stimulus	−4.3	−17	−12
AK002622	Pln	phospholamban	regulation of the force of heart contraction /// calcium ion transport /// regulation of calcium ion transport	−2.2	−3.3	−2.2
AK002622	Pln	phospholamban	regulation of the force of heart contraction /// calcium ion transport /// regulation of calcium ion transport	−3.0	−5.3	−3.2
BC010288	Psp	parotid secretory protein	—	−6.4	−18	−62
NM_007389	Chrna1	cholinergic receptor, nicotinic, alpha polypeptide 1 (muscle)	ion transport /// neuromuscular synaptic transmission /// regulation of membrane potential	−2.2	−3.2	−3.4
BB020678	Fam196b	family with sequence similarity 196, member B	—	−2.9	−7.0	−16
AV026232	4832428D23Rik	RIKEN cDNA 4832428D23 gene	—	−2.1	−2.1	−4.1

Table 3. Validation of Differentially Expressed Genes by Real-Time PCR Fold Changes of Transcripts from Microarray VS from Real-Time PCR

	3w microarray	*3w real-time PCR*	*6w microarray*	*6w real-time PCR*	*3m microarray*	*3m real-time PCR*
Upregulated genes						
Kcne1l	2.2	2.6 ± 0.1	4.4	3.8 ± 1	6.1	3.2 ± 0.3
Myom2	5.0	8.3 ± 1.0	14	22 ± 3	16	23 ± 1
Ryr3	3.2	5.5 ± 0.8	5.8	5.3 ± 0.8	7.9	10 ± 2
Zmynd17	5.4	25 ± 1	22	27 ± 3	18	26 ± 4
Downregulated genes						
Cacna2d4	−4.3	−6.9 ± 0.3	−17	−35 ± 7	−12	−34 ± 2
Myh6	−6.4	−15 ± 2	−14	−8.4 ± 0.6	−6.3	−6.2 ± 0.7
Myh7	−3.1	−4.6 ± 0.1	−6.5	−6.9 ± 0.3	−10	−6.1 ± 0.5
Myl2	−4.3	−7.4 ± 0.3	−7.9	−17 ± 4	−7.1	−9.3 ± 0.7
Pln	−3.0	−2.4 ± 0.2	−5.3	−3.9 ± 0.2	−3.2	−3.7 ± 0.2
Psp	−6.4	−6.4 ± 0.2	−18	−39 ± 3	−62	−273 ± 8
Tnnc1	−3.7	−5.3 ± 0.2	−8.8	−6.2 ± 0.1	−12	−12 ± 0.2
Tnni1	−5.6	−9.5 ± 0.3	−18	−22 ± 1	−24	−24 ± 1
Tnnt2	−4.1	−5.6 ± 0.4	−19	−14 ± 2	−11	−11 ± 1
Zfp533	−2.7	−3.3 ± 0.1	−5.1	−21 ± 1	−6.2	−6.4 ± 0.6

Myosin Heavy Chain and Related Genes

We have previously detailed the gene and protein expression patterns of myosin heavy chains in wild-type and *Pitx2*-deficient EOMs.[13,26] Of the nine myosin heavy chain isoforms expressed in EOMs, four of them (*Myh6*, *Myh7*, *Myh13*, and *Myh14*) exhibited a dramatic decrease in the expression of both transcript and protein levels, whereas *Myh1* and *Myh2* had altered cross-sectional and longitudinal expression patterns, although the transcript levels did not show a significant change. Our current genomic profiling demonstrated that *Myh6* and *Myh7* transcripts were dramatically reduced, as were transcripts of troponins expected to bind these myosin heavy chains,[27] whereas transcript levels for *Myh1*, *Myh2*, *Myh3*, and *Myh4* were not significantly altered (data not shown), supporting our previous data with qPCR and immunohistochemistry.[12,13] *Myh13* and *Myh14*, which are expressed in EOMs,[28,29] were not represented on the gene chips used for this investigation.

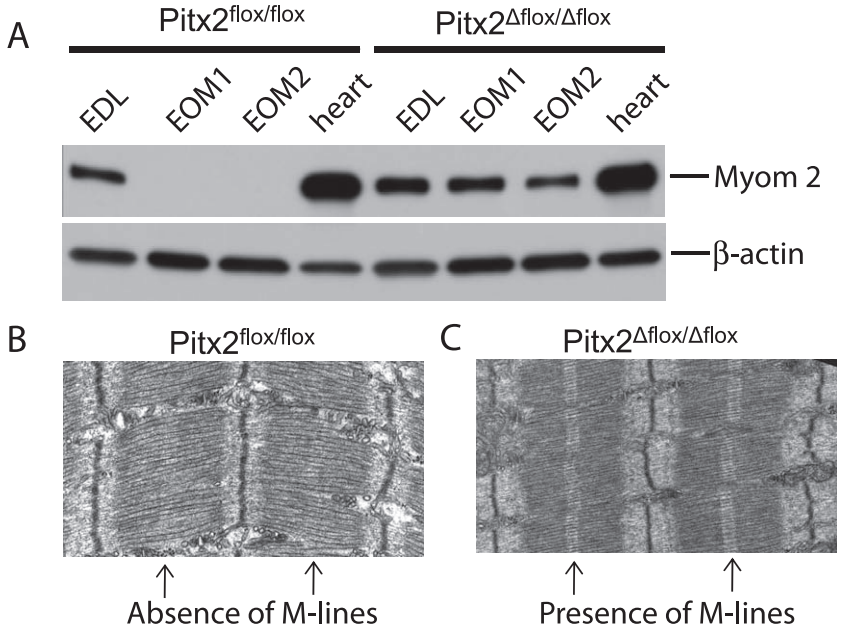

Figure 3. Validation of myomesin 2 expression in *Pitx2*$^{\Delta flox/\Delta flox}$ extraocular muscle. Western blot analysis (**A**) showed that myomesin 2 is not expressed in *Pitx2*$^{flox/flox}$ extraocular muscle but readily detected in the *Pitx2*$^{\Delta flox/\Delta flox}$ extraocular muscle. This upregulation is unique to extraocular muscle as myomesin 2 is expressed in both extensor digitorum longus and heart at comparable levels between *Pitx2*$^{\Delta flox/\Delta flox}$ and *Pitx2*$^{flox/flox}$ mice. Duplicate samples of EOM tissues from two different mice of both *Pitx2*$^{\Delta flox/\Delta flox}$ and *Pitx2*$^{flox/flox}$ genotypes were used for Western blot analysis. Electron microscopy showed that sarcomeres of the extraocular muscles from the *Pitx2*$^{flox/flox}$ mice (**B**) do not have M-lines, whereas that from *Pitx2*$^{\Delta flox/\Delta flox}$ mice (**C**) now have M-lines.

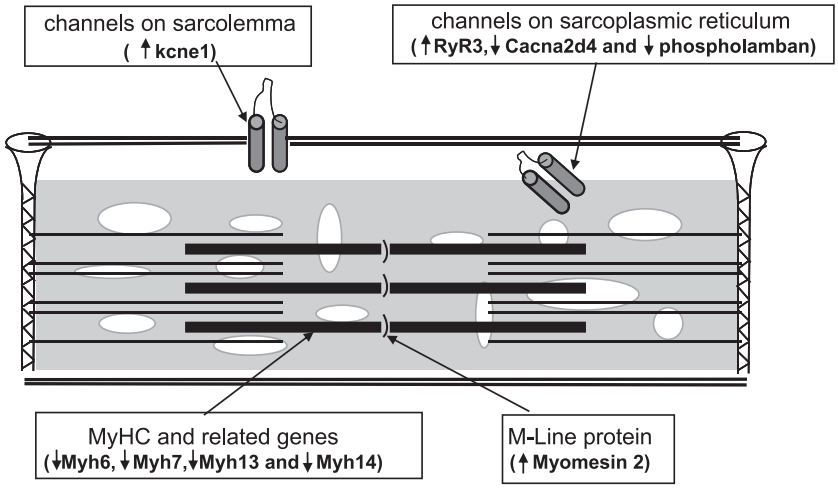

Figure 4. Schematic representation of key gene expression alterations that are associated with the conditional knockout of *Pitx2* in EOM. The transcript alterations are consistent with the physiologic alterations that would produce a muscle that has greater contractile force and speed, which is consistent with previous physiologic studies (see Discussion section for details).

Structural Proteins

The sarcomere is the functional and structural unit for the striated musculature, in which the thin actin filaments and the thick myosin filaments are arranged into an orderly lattice.[23] Myomesin 1 and myomesin 2 are the principal scaffolding components of M-lines, which cross-link the thick filaments in sarcomeres. M-lines tend to be most prominent in fast-twitch muscle fibers and myomesin 2 is found exclusively in fast-twitch fibers.[22,23] Myomesin 2 is thought to improve the stability of thick filament lattices by increasing their stiffness and thus increasing their force generation.[30] After early developmental stages of EOM, myomesin expression is downregulated,[31,32] and sarcomeres develop a "fuzzy" appearance, weaker M-bands, and poor lattice order. Despite their rapid contractile characteristics, adult EOM fibers of rodents do not express myomesin 2 and lack well-structured M-lines typical of other skeletal muscle.[24,31,33] Wiesen and colleagues[24] hypothesized that the poor lattice structure of sarcomeres lacking M-line components in EOM would contribute to the fibers being more elastic and having lower force generation.[24,34,35] In the *Pitx2*$^{\Delta flox/\Delta flox}$ mice, myomesin 2 transcripts were found to be significantly increased in the genomic profile. The profiling observations were verified by qPCR and immunoblot analysis. Ultrastructural analysis was focused on orbital region fibers, since they are known to have a particularly poorly defined M-line structure, whereas global region fibers are much more heterogeneous.[24] Interestingly, M-lines were identified in fibers of the *Pitx2*-deficient mice but not in the *Pitx2*$^{flox/flox}$ mice. Previous physiological studies[12] of EOM from *Pitx2*$^{\Delta flox/\Delta flox}$ mice identified the muscles to have greater force generation, which would support the contention espoused by Wiesen and colleagues[24]that mature M-line structures would enhance force generation.

Channel and Transport

Across the three time points we found the transcript for the potassium channel ancillary protein Kcne1 to be increased in expression in the *Pitx2*$^{\Delta flox/\Delta flox}$ EOM. KCNE peptides influence expression, pharmacology, and physiologic properties of potassium channels.[36] KCNE1 slows voltage-stimulated channel activation, increases conductance, and eliminates channel inactivation.[37,38] The expectation of KCNE1 upregulation in the *Pitx2*$^{\Delta flox/\Delta flox}$ EOM would be to terminate muscle depolarization more rapidly, producing a more rapid twitch contraction, which is what we have observed.[12]

The expression of ryanodine receptor 3 (*RyR3*) was also found to gradually increase over time. The *RyR3* gene encodes the intracellular Ca^{2+} release channel ryanodine receptor.[39] Together, RyR3 along with RyR1 control the resting calcium ion concentration in skeletal muscle.[40] Enhanced expression of RyR3 would be expected to lead to more rapid calcium sequestration and a shorter twitch, which is what we observed in Pitx2-deficient EOM. *Cacna2d4* encodes an L-type calcium channel auxiliary subunit gene.[41] In skeletal muscle, opening of the L-type calcium channel in the sarcoplasmic reticulum (SR) causes opening of the ryanodine receptor. Calcium released from the SR binds to troponin C on the actin filaments as part of activation of muscle contraction. In human embryonic kidney 293 cells, the *Cacna2d4* subunit increases calcium influx.[41] If the same occurs in EOM, the reduced expression of *Cacna2d4* in the Pitx2-deficient mice may lead to a shorter period of contraction. Phospholamban interacts with the SR calcium pump (SERCA) and decreases SERCA calcium affinity, thereby reducing contractile force.[42] Phospholamban is preferentially expressed in slow-twitch fibers.[43] The Ca affinity for Ca transport of SERCA 1 or 2, both of which are expressed in EOM, is lowered by coexpression with phospholamban.[44] Here again, the reduction of phospholamban expression would serve to increase the force of contraction, which is exactly what was observed in our previous contractile studies.

The gene transcript encoding the α-subunit of acetylcholine receptor was reduced in the *Pitx2*-deficient EOM. Our previous investigation[13] identified loss of multiinnervation, which likely explains the reduced production of the α-subunit transcript.

Transcriptional Factors

We identified alterations in transcriptional factors (*Zmynd17*, *Zdhhc23*, *Zfp385b*), each of which have zinc finger domains. Although it is known that Zfp385b is expressed in heart and ocular tissues,[45] the function of these transcription factors is otherwise unknown. Their differential expression is influenced

by *Pitx2* deficiency and presumably has a functional role in influencing the mature EOM phenotype.

Cortexin 3

Cortexin 3 was found upregulated across all three time points of investigation. Previously, identified only in kidney and brain,[46] cortexin 3 has been found to promote neurite growth in culture.[47] A highly speculative interpretation of this observation would be that cortexin 3 upregulation is a response to the loss of multiinnervation in the *Pitx2*-deficient EOM and is an attempt to induce neurite outgrowth.

Conclusions

Our investigations indicate that Pitx2 in the mature EOM regulates a subset of genes primarily related to muscle contraction (Fig. 4). From the present evaluation, we cannot determine whether Pitx2 directly regulates transcription of these genes or whether it acts through intermediaries. The alteration of contractile characteristics and multiinnervation is also likely to influence gene expression indirectly in the EOM of $Pitx2^{\Delta flox/\Delta flox}$ mice. Further definition of transcription regulation of the adult EOM phenotype will allow a logical manipulation of gene transcription, to modify EOM contraction for therapeutic purposes.

References

1. Spencer RF, Porter JD. Biological organization of the extraocular muscles. *Prog Brain Res*. 2006;151:43–80.
2. Kaminski HJ, Richmonds CR, Kusner LL, Mitsumoto H. Differential susceptibility of the ocular motor system to disease. *Ann NY Acad Sci*. 2002;956:42–54.
3. Gundersen K, Leberer E, Lomo T, Pette D, Staron RS. Fibre types, calcium-sequestering proteins and metabolic enzymes in denervated and chronically stimulated muscles of the rat. *J Physiol*. 1988;398:177–189.
4. Goldspink G, Scutt A, Loughna PT, Wells DJ, Jaenicke T, Gerlach GF. Gene expression in skeletal muscle in response to stretch and force generation. *Am J Physiol*. 1992;262:R356–363.
5. Goldspink G, Scutt A, Martindale J, Jaenicke T, Turay L, Gerlach GF. Stretch and force generation induce rapid hypertrophy and myosin isoform gene switching in adult skeletal muscle. *Biochem Soc Trans*. 1991;19:368–373.
6. Simonides WS, van Hardeveld C. Thyroid hormone as a determinant of metabolic and contractile phenotype of skeletal muscle. *Thyroid*. 2008;18:205–216.
7. Gage PJ, Suh H, Camper SA. Dosage requirement of Pitx2 for development of multiple organs. *Development*. 1999;126:4643–4651.
8. Lin CR, Kioussi C, O'Connell S, et al. Pitx2 regulates lung asymmetry, cardiac positioning and pituitary and tooth morphogenesis. *Nature*. 1999;401:279–282.
9. Piedra ME, Icardo JM, Albajar M, Rodriguez-Rey JC, Ros MA. Pitx2 participates in the late phase of the pathway controlling left-right asymmetry. *Cell*. 1998;94:319–324.
10. Ryan AK, Blumberg B, Rodriguez-Esteban C, et al. Pitx2 determines left-right asymmetry of internal organs in vertebrates. *Nature*. 1998;394:545–551.
11. Kitamura K, Miura H, Miyagawa-Tomita S, et al. Mouse Pitx2 deficiency leads to anomalies of the ventral body wall, heart, extra- and periocular mesoderm and right pulmonary isomerism. *Development*. 1999;126:5749–5758.
12. Zhou Y, Cheng G, Dieter L, et al. An altered phenotype in a conditional knockout of Pitx2 in extraocular muscle. *Invest Ophthalmol Vis Sci*. 2009;50:4531–4541.
13. Zhou Y, Liu D, Kaminski HJ. Pitx2 regulates myosin heavy chain isoform expression and multi-innervation in extraocular muscle. *J Physiol*. 2011;589:4601–4614.
14. Fischer MD, Gorospe JR, Felder E, et al. Expression profiling reveals metabolic and structural components of extraocular muscles. *Physiol Genomics*. 2002;9:71–84.
15. Porter JD, Khanna S, Kaminski HJ, et al. Extraocular muscle is defined by a fundamentally distinct gene expression profile. *Proc Natl Acad Sci U S A*. 2001;98:12062–12067.
16. Porter JD, Khanna S, Kaminski HJ, et al. A chronic inflammatory response dominates the skeletal muscle molecular signature in dystrophin-deficient mdx mice. *Hum Mol Genet*. 2002;11:263–272.
17. Porter JD, Merriam AP, Leahy P, Gong B, Khanna S. Dissection of temporal gene expression signatures of affected and spared muscle groups in dystrophin-deficient (mdx) mice. *Hum Mol Genet*. 2003;12:1813–1821.
18. Pfaffl MW. A new mathematical model for relative quantification in real-time RT-PCR. *Nucleic Acids Res*. 2001;29:e45.
19. Talmadge RJ, Roy RR. Electrophoretic separation of rat skeletal muscle myosin heavy-chain isoforms. *J Appl Physiol*. 1993;75:2337–2340.
20. Bradford MM. A rapid and sensitive method for the quantitation of microgram quantities of protein utilizing the principle of protein-dye binding. *Anal Biochem*. 1976;72:248–254.
21. Schneiter R, Hitomi M, Ivessa AS, Fasch EV, Kohlwein SD, Tartakoff AM. A yeast acetyl coenzyme A carboxylase mutant links very-long-chain fatty acid synthesis to the structure and function of the nuclear membrane-pore complex. *Mol Cell Biol*. 1996;16:7161–7172.
22. Squire JM. Architecture and function in the muscle sarcomere. *Curr Opin Struct Biol*. 1997;7:247–257.
23. Agarkova I, Perriard JC. The M-band: an elastic web that crosslinks thick filaments in the center of the sarcomere. *Trends Cell Biol*. 2005;15:477–485.
24. Wiesen MH, Bogdanovich S, Agarkova I, Perriard JC, Khurana TS. Identification and characterization of layer-specific differences in extraocular muscle M-bands. *Invest Ophthalmol Vis Sci*. 2007;48:1119–1127.
25. English AW, Wolf SL. The motor unit. Anatomy and physiology. *Phys Ther*. 1982;62:1763–1772.
26. Zhou Y, Liu D, Kaminski HJ. Myosin heavy chain expression in mouse extraocular muscle: more complex than expected. *Invest Ophthalmol Vis Sci*. 2010;51:6355–6363.
27. Gomes AV, Potter JD, Szczesna-Cordary D. The role of troponins in muscle contraction. *IUBMB Life*. 2002;54:323–333.
28. Schachat F, Briggs MM. Phylogenetic implications of the superfast myosin in extraocular muscles. *J Exp Biol*. 2002;205:2189–2201.
29. Rossi AC, Mammucari C, Argentini C, Reggiani C, Schiaffino S. Two novel/ancient myosins in mammalian skeletal muscles: MYH14/7b and MYH15 are expressed in extraocular muscles and muscle spindles. *J Physiol*. 2010;588:353–364.
30. Pask HT, Jones KL, Luther PK, Squire JM. M-band structure, M-bridge interactions and contraction speed in vertebrate cardiac muscles. *J Muscle Res Cell Motil*. 1994;15:633–645.
31. Porter JD, Merriam AP, Gong B, et al. Postnatal suppression of myomesin, muscle creatine kinase and the M-line in rat extraocular muscle. *J Exp Biol*. 2003;206:3101–3112.
32. Fischer MD, Budak MT, Bakay M, et al. Definition of the unique human extraocular muscle allotype by expression profiling. *Physiol Genomics*. 2005;22:283–291.
33. Andrade FH, Merriam AP, Guo W, et al. Paradoxical absence of M lines and downregulation of creatine kinase in mouse extraocular muscle. *J Appl Physiol*. 2003;95:692–699.

34. Agarkova I, Ehler E, Lange S, Schoenauer R, Perriard JC. M-band: a safeguard for sarcomere stability? *J Muscle Res Cell Motil*. 2003;24:191–203.
35. Agarkova I, Schoenauer R, Ehler E, et al. The molecular composition of the sarcomeric M-band correlates with muscle fiber type. *Eur J Cell Biol*. 2004;83:193–204.
36. Roura-Ferrer M, Etxebarria A, Sole L, et al. Functional implications of KCNE subunit expression for the Kv7.5 (KCNQ5) channel. *Cell Physiol Biochem*. 2009;24:325–334.
37. McCrossan ZA, Abbott GW. The MinK-related peptides. *Neuropharmacology*. 2004;47:787–821.
38. Melman YF, Krummerman A, McDonald TV. KCNE regulation of KvLQT1 channels: structure-function correlates. *Trends Cardiovasc Med*. 2002;12:182–187.
39. Lanner JT, Georgiou DK, Joshi AD, Hamilton SL. Ryanodine receptors: structure, expression, molecular details, and function in calcium release. *Cold Spring Harb Perspect Biol*. 2010;2:a003996.
40. Perez CF, Lopez JR, Allen PD. Expression levels of RyR1 and RyR3 control resting free Ca^{2+} in skeletal muscle. *Am J Physiol Cell Physiol*. 2005;288:C640–C649.
41. Qin N, Yagel S, Momplaisir ML, Codd EE, D'Andrea MR. Molecular cloning and characterization of the human voltage-gated calcium channel alpha(2)delta-4 subunit. *Mol Pharmacol*. 2002;62:485–496.
42. Mueller B, Karim CB, Negrashov IV, Kutchai H, Thomas DD. Direct detection of phospholamban and sarcoplasmic reticulum Ca-ATPase interaction in membranes using fluorescence resonance energy transfer. *Biochemistry*. 2004;43:8754–8765.
43. Jorgensen AO, Jones LR. Localization of phospholamban in slow but not fast canine skeletal muscle fibers. An immunocytochemical and biochemical study. *J Biol Chem*. 1986;261:3775–3781.
44. Kjellgren D, Ryan M, Ohlendieck K, Thornell LE, Pedrosa-Domellof F. Sarco(endo)plasmic reticulum Ca^{2+} ATPases (SERCA1 and -2) in human extraocular muscles. *Invest Ophthalmol Vis Sci*. 2003;44:5057–5062.
45. Strausberg RL, Feingold EA, Grouse LH, et al. Generation and initial analysis of more than 15,000 full-length human and mouse cDNA sequences. *Proc Natl Acad Sci U S A*. 2002;99:16899–16903.
46. Wang HT, Chang JW, Guo Z, Li BG. In silico-initiated cloning and molecular characterization of cortexin 3, a novel human gene specifically expressed in the kidney and brain, and well conserved in vertebrates. *Int J Mol Med*. 2007;20:501–510.
47. Chalisova NI, Khavinson VK. Studies of cytokines in nerve tissue cultures. *Neurosci Behav Physiol*. 2000;30:261–265.